

$\psi(3770)$ resonance and its production in $\bar{p}p \rightarrow D\bar{D}$ J. Haidenbauer¹ and G. Krein²¹*Institute for Advanced Simulation and Jülich Center for Hadron Physics,
Forschungszentrum Jülich, D-52425 Jülich, Germany*²*Instituto de Física Teórica, Universidade Estadual Paulista, Rua Dr. Bento Teobaldo Ferraz,
271—01140-070 São Paulo, São Paulo, Brazil*

(Received 4 May 2015; published 17 June 2015)

The production of a $D\bar{D}$ meson pair in antiproton-proton ($\bar{p}p$) annihilation close to the production threshold is investigated, with special emphasis on the role played by the $\psi(3770)$ resonance. The study is performed in a meson-baryon model where the elementary charm production process is described by baryon exchange. Effects of the interactions in the initial and final states are taken into account rigorously, where the latter involves also those due to the $\psi(3770)$. The predictions for the $D\bar{D}$ production cross section are in the range of 30–250 nb, and the contribution from the $\psi(3770)$ resonance itself amounts to roughly 20–80 nb.

DOI: 10.1103/PhysRevD.91.114022

PACS numbers: 13.60.Le, 14.40.Lb, 25.43.+t

I. INTRODUCTION

In a recent publication [1], we presented predictions for the charm-production reaction $\bar{p}p \rightarrow D\bar{D}$ close to the threshold based on a model where the elementary charm production process is described by baryon exchange and also in the constituent quark model. The cross section was found to be in the order of 10–100 nb, and it turned out to be comparable to those predicted by other model calculations in the literature [2–7].

The results in Ref. [1] suggested that the reaction $\bar{p}p \rightarrow D\bar{D}$ takes place predominantly in the s wave, at least for excess energies below 100 MeV. However, there is a well-established p -wave resonance, the $\psi(3770)$ ($J^{\text{PC}} = 1^{--}$), which is seen as a pronounced structure in $e^+e^- \rightarrow D\bar{D}$ [8,9], for example, and which is located at only around 35 MeV above the $D\bar{D}$ threshold. The resonance decays almost exclusively (i.e., to 93⁺⁸₋₉%) into $D\bar{D}$ [10]. This resonance was not included in our previous study [1]. Given its apparent prominence in the $D\bar{D}$ channel, the impact of the $\psi(3770)$ on the $\bar{p}p \rightarrow D\bar{D}$ cross section clearly should be explored. In particular, should it turn out that its contribution is rather large, then it would be certainly interesting to examine the energy range in question in pertinent experiments, which could be performed by the PANDA Collaboration [11–13] at the future Facility for Antiproton and Ion Research (FAIR) in Darmstadt.

In the present study, we consider the effect of the $\psi(3770)$ on the $\bar{p}p \rightarrow D\bar{D}$ cross section. The work complements our results presented in Ref. [1] and builds on the Jülich meson-baryon model for the reaction $\bar{p}p \rightarrow \bar{K}K$ [14] where the extension of the model from the strangeness to the charm sector follows a strategy similar to other studies by us on the DN and $\bar{D}N$ interactions [15–17], and on the reaction $\bar{p}p \rightarrow \bar{\Lambda}_c^-\Lambda_c^+$ [18], namely by assuming as a working hypothesis SU(4) symmetry constraints.

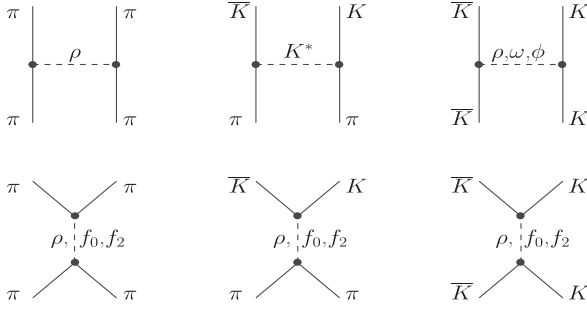
II. MODEL

The framework in which we treat the charm-production reaction $\bar{p}p \rightarrow D\bar{D}$ is described in detail in Ref. [1]. Here we summarize only the principal features. The reaction amplitude for $\bar{p}p \rightarrow D\bar{D}$ is obtained within the distorted-wave Born approximation. Effects of the initial-state interaction (ISI) as well as of the final-state interaction (FSI), which play an important role for energies near the production threshold [19,20], are taken into account rigorously. The employed $\bar{N}N$ and $D\bar{D}$ amplitudes are solutions of Lippmann–Schwinger-type scattering equations based on corresponding ($\bar{N}N$ and $D\bar{D}$) interaction potentials.

The microscopic charm-production process itself is described by baryon exchange (Λ_c, Σ_c), in close analogy to an investigation of the strangeness production reaction $\bar{p}p \rightarrow \bar{K}K$ by the Jülich group [14]. Specifically, the transition potential is derived from the corresponding transition in the $\bar{K}K$ case under the assumption of SU(4) symmetry; see Ref. [1] for details.

Because of the known sensitivity of the results for the cross sections on the initial $\bar{p}p$ interaction, we examined its effect by considering several variants of the $\bar{N}N$ potential. Details of those potentials can be found in Refs. [1,18]. Here we just want to mention that they differ primarily in the elastic part where we consider variations from keeping only the longest-ranged contribution (one-pion exchange) to taking a full G-parity transformed NN interaction as done in Ref. [19]. All those models reproduce the total $\bar{p}p$ cross section in the relevant energy range and, in general, describe also data on integrated elastic and charge-exchange cross sections and even $\bar{p}p$ differential cross sections, cf. Refs. [1,18].

The interaction in the $D\bar{D}$ system is constructed along the lines of the Jülich meson exchange model for the $\pi\pi$

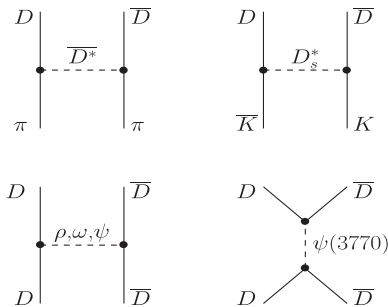
FIG. 1. Diagrams included in the Jülich $\pi\pi - K\bar{K}$ potential [22].

interaction of which the evaluation has been discussed in detail in Refs. [21,22]. The present interaction is based on the version described in the latter reference. The potentials for $\pi\pi \rightarrow \pi\pi$, $\pi\pi \rightarrow K\bar{K}$ and $K\bar{K} \rightarrow K\bar{K}$ are generated from the diagrams shown in Fig. 1. The additional diagrams that arise for the $D\bar{D}$ potential and for the transitions from $\pi\pi$ and/or $K\bar{K}$ to $D\bar{D}$ are shown in Fig. 2. In this extension we were guided by SU(4) symmetry [1]. Thus, we included t -channel exchanges of those vector mesons which are from the same SU(4) multiplet as those included in the original Jülich model, and, moreover, we assumed that all coupling constants at the additional three-meson vertices are given by SU(4) relations. Indeed, in Ref. [1] an even more extended model was considered which included also the coupling to channels involving the charmed strange meson $D_s(1969)$. It turned out that the $D\bar{D}$ production cross sections based on the $D\bar{D}$ interactions with or without coupling to $D_s^+ D_s^-$ are almost identical, and therefore, in the present work, we show only the results for the latter case. The parameters of the model can be found in Appendix C of Ref. [1].

The scattering amplitudes are obtained by solving a coupled channel scattering equation for these potentials which is formally given by

$$T^{i,j} = V^{i,j} + \sum_l V^{i,l} G^l T^{l,j}, \quad (1)$$

with $i, j, l = \pi\pi, \pi\eta, \bar{K}K, D\bar{D}$.

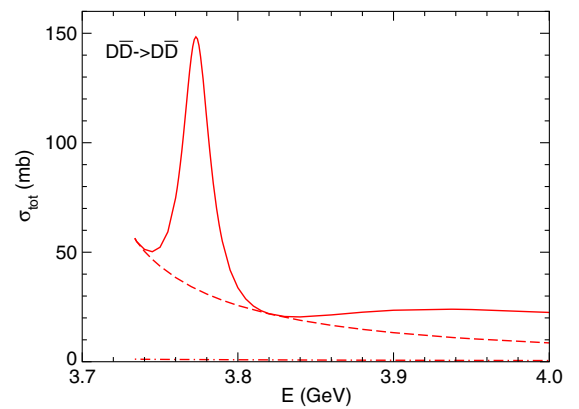
FIG. 2. Additional diagrams that arise when the $D\bar{D}$ channel is included.

In an approach like ours, the $\psi(3770)$ (in the following usually called ψ to simplify the notation) has to be included as bare resonance. It acquires its physical mass and its width when the corresponding potential is iterated in the scattering equation (1). We include the ψ only in the direct $D\bar{D}$ potential, i.e., in $V^{D\bar{D},D\bar{D}}$. The corresponding diagram is depicted on the lower right side of Fig. 2. The potential can be written in the form

$$V^{D\bar{D},D\bar{D}} = \gamma_0^{D\bar{D}} \frac{1}{E - m_0} \gamma_0^{D\bar{D}}, \quad (2)$$

with a bare $D\bar{D}\psi$ vertex function $\gamma_0^{D\bar{D}}$ and a bare $\psi(3770)$ mass m_0 . Explicit expressions for the vertex function of two pseudoscalar mesons coupled to a vector meson in the s -channel and for the resulting potential can be found in the Appendix of Ref. [22]. The bare mass m_0 and the bare coupling constant in $\gamma_0^{D\bar{D}}$ are adjusted in such a way that the resulting T -matrix, $T^{D\bar{D},D\bar{D}}$, has a pole at the physical values of the $\psi(3770)$ resonance. The main results shown in the present study are based on a $D\bar{D}$ model that produces a pole at $E = (3773 - i13.6)$ MeV, i.e., at the value specified as “our fit” by the Particle Data Group (PDG) [10], but we consider also the value obtained in Ref. [9] for the mass which is about 6 MeV larger. In the actual calculation, the values for the mass and width of the $\psi(3770)$ were determined by evaluating the speed plot for $T^{D\bar{D},D\bar{D}}$ for simplicity reasons. In addition, we use an isospin averaged mass for the D (\bar{D}), namely, 1866.9 MeV. The bare masses and bare coupling constants of the $\psi(3770)$ are 3860.2 MeV and 0.4901 and 3884.2 MeV and 0.6801, respectively, in the convention of Ref. [22].

Cross sections for $D\bar{D}$ scattering in the isospin $I = 0$ and $I = 1$ states can be found in Fig. 3. For the $I = 0$ case, we show the result from the s wave separately (dashed curve) so that one can see the impact due to the $\psi(3770)$

FIG. 3 (color online). Total cross section for $D\bar{D}$ scattering as a function of the center-of-mass energy for isospin $I = 0$ (solid line) and $I = 1$ (dash-dotted line). The s -wave contribution to the $I = 0$ cross section is indicated by the dashed line.

resonance. Note that there is actually an appreciable nonresonant contribution in the p wave which is clearly visible for energies away from the $\psi(3770)$, i.e., around 3.9 GeV and above. The cross section in the $I = 1$ state is very small. It is only in the order of 1 mb and, therefore, hardly recognizable in Fig. 3. This rather different behavior can be easily understood if one recalls that for $I = 0$ the contributions of the vector mesons (ρ , ω , J/ψ) all add coherently and provide a strong attractive force. In the $I = 1$ channel, the contribution from ρ exchange is of opposite sign, and, thus, the interaction due to the ρ and those by ω and J/ψ exchange cancel to a large extent, and the resulting potential is fairly weak. Indeed, the very same situation occurs in the $\bar{K}K$ system as discussed in Ref. [22]. In this context let us mention that there are other model results on the $D\bar{D}$ interaction in the literature [23], achieved likewise in a meson-exchange approach.

For completeness reasons we present here also results for the reaction $e^+e^- \rightarrow D\bar{D}$, cf. Fig. 4. Results corresponding to a ψ mass of 3773 or 3779 MeV, respectively, are indicated by the thick and thin solid lines. The pertinent calculation was performed in the Migdal–Watson approximation [24,25], i.e., by assuming that $T^{D\bar{D},e^+e^-} \propto T^{D\bar{D},D\bar{D}}$, so that the cross section for $e^+e^- \rightarrow D\bar{D}$ is given by

$$\sigma_{e^+e^- \rightarrow D\bar{D}} \approx N q_{D\bar{D}} |T^{D\bar{D},D\bar{D}}|^2. \quad (3)$$

Here $q_{D\bar{D}}$ is the $D\bar{D}$ center-of-mass momentum, and N is an arbitrary normalization factor that has to be adjusted to the data. The shown curve is based on the $D\bar{D}I = 0$ amplitude in the p wave. In this case a factor $q_{D\bar{D}}^2$ has to be divided out because in $e^+e^- \rightarrow D\bar{D}$ the incoming $D\bar{D}$ state is not on shell and, therefore, does not feel the angular-momentum threshold factor [26].

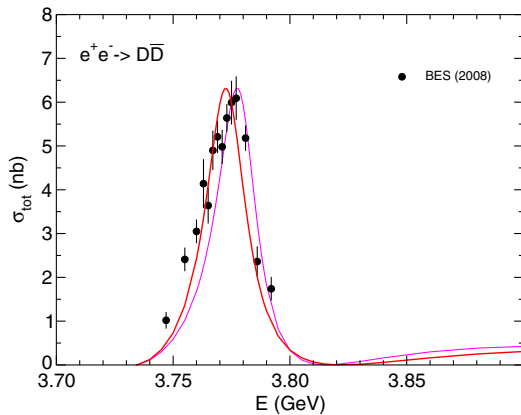


FIG. 4 (color online). Integrated cross sections for $e^+e^- \rightarrow D\bar{D}$. Our results based on the Migdal–Watson approximation are shown by the thick solid line ($m_\psi = 3773$ MeV) and the thin solid line ($m_\psi = 3779$ MeV). Data are taken from Ref. [8].

Our result is in remarkably good agreement with the measured line shape. In particular, the strong falloff after the peak value is very well described. Note that the symbols in Fig. 4 represent the combined $(D^+D^-, D^0\bar{D}^0)$ results of the measurement by the BES collaboration as given in the last column of Table 2 of Ref. [8]. Since there is no isospin breaking in our hadronic interaction, the spectra produced for the D^+D^- and $D^0\bar{D}^0$ final states are identical within the employed Migdal–Watson approximation (3). Specifically, the quantitative differences in the line shape with regard to the experiment, visible in Fig. 4, are also present in the individual channels. Let us emphasize, however, that in any case one has to expect that the signal of the $\psi(3770)$ in $D\bar{D} \rightarrow D\bar{D}$ or $\bar{p}p \rightarrow D\bar{D}$ should differ quantitatively from the one seen in the $e^+e^- \rightarrow D\bar{D}$ reactions, simply because the nonresonant contributions that provide the so-called background are necessarily different in different reactions.

As mentioned, we adjusted our resonance parameters to the “our fit” value of the PDG. No fine-tuning to the actual ($e^+e^- \rightarrow D^+D^-$ and $e^+e^- \rightarrow D^0\bar{D}^0$) data was done because we are primarily interested in studying the effect of the $\psi(3770)$ on $\bar{p}p \rightarrow D\bar{D}$ observables and not in pinning down its resonance parameters. In particular, it is not the aim of the present work to resolve the uncertainty in the order of 6 MeV with regard to the actual resonance mass [9,10]. For dedicated analyses of the $e^+e^- \rightarrow D\bar{D}$ data, see Refs. [8,9,23,27–30].

III. RESULTS FOR THE REACTION $\bar{p}p \rightarrow D\bar{D}$

Results for the reaction $\bar{p}p \rightarrow D\bar{D}$ are presented in Figs. 5 and 6. We employ again all $\bar{p}p$ ISI considered in our previous work [1]. As noted before, the ISI introduces by far the largest uncertainty into our calculation, and in order to indicate this uncertainty, we displayed the results as bands in Ref. [1]. We refrain from showing such bands here because we want to highlight the impact of the $\psi(3770)$, and this information would have been otherwise hidden in the band. Nonetheless, the variations due to the ISI and the uncertainty implied by it can be still read off from the Figs. 5 and 6 because we present curves corresponding to the largest and smallest predictions for the $\bar{p}p \rightarrow D^0\bar{D}^0$ and $\bar{p}p \rightarrow D^+D^-$ cross sections.

The solid and dash-dotted lines in Figs. 5 and 6 are results with inclusion of the $\psi(3770)$ resonance, while the dashed and dotted curves are based on the $D\bar{D}$ FSI without the ψ , i.e., corresponding to the case considered already in Ref. [1]. Please recall that in our calculation the ψ is only included in the $D\bar{D}$ interaction and, therefore, its effects come exclusively from the corresponding FSI. In principle, there could be also a coupling of the (bare) ψ to the $\bar{N}N$ system which would then contribute to the $\bar{p}p \rightarrow D\bar{D}$ transition potential. However, we assume here that this possible coupling is negligibly small—because it is suppressed by the Okubo–Zweig–Iizuka rule (OZI). After all, it requires the

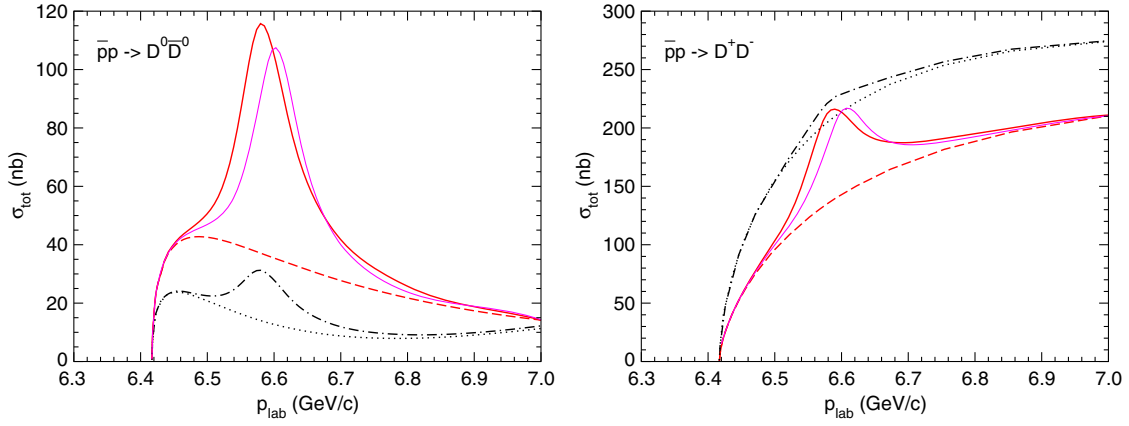


FIG. 5 (color online). Total reaction cross sections for $\bar{p}p \rightarrow D\bar{D}$ as a function of p_{lab} . The (red) solid and dashed curves and the (black) dash-dotted and dotted curves are results for different $\bar{p}p$ initial-state interactions; see the text. Solid and dash-dotted curves show the full results with inclusion of the $\psi(3770)$ in the FSI, while dashed and dotted curves are without $\psi(3770)$. The (magenta) thin solid curves indicate results based on a $D\bar{D}$ FSI fitted to the higher ψ mass (3779 MeV) obtained in Ref. [9].

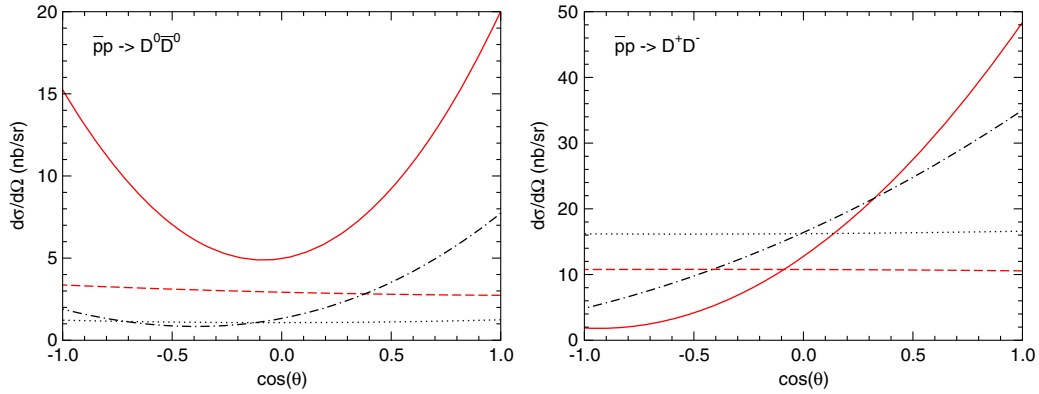


FIG. 6 (color online). Differential cross sections for $\bar{p}p \rightarrow D\bar{D}$ at $p_{\text{lab}} = 6.578$ GeV/c (excess energy $\epsilon = 40$ MeV). The same description of curves as in Fig. 5.

annihilation of three up- and/or down-quark pairs and the creation of a $c\bar{c}$ quark pair; see the discussion in Sec. IV.

It is obvious that the $\psi(3770)$ resonance leads to a pronounced enhancement in the $D\bar{D}$ production cross section. Especially, for the $D^0\bar{D}^0$ final state, the cross section predicted around the resonance peak is now practically twice as large. Quantitatively, our calculation suggests that the cross section due to the $\psi(3770)$ resonance could be the order of 20 to 80 nb. The effect is less dramatic in the D^+D^- case because here the s -wave contributions are fairly large. Still for both reactions there should be good chances that one can see a clear resonance signal over the background (that comes mostly from the s wave) in an actual experiment.

A comparison of the two results with and of the two without $\psi(3770)$ resonance (solid vs dash-dotted line or dashed vs dotted line, respectively) in Fig. 5 allows one to see the uncertainties in the predictions due to the employed $\bar{p}p$ interactions. Those are substantial but not really

dramatic as already discussed in Ref. [1]. There is a somewhat larger uncertainty with regard to the contribution of the $\psi(3770)$ resonance which, however, is not too surprising. Conservation of total angular momentum and parity implies that the $D\bar{D}$ s wave is produced from the $\bar{N}N$ 3P_0 partial wave while the $D\bar{D}$ p wave is produced from the $\bar{N}N$ 3S_1 - 3D_1 partial wave. Since the 3S_1 partial wave is much more sensitive to short-range physics than higher partial waves, there is also a stronger variation in the corresponding amplitudes for the various $\bar{N}N$ potentials considered as ISI.

The thin solid lines indicate what happens if we employ a $D\bar{D}$ FSI that is fitted to the higher value given for the $\psi(3770)$ resonance, i.e., to 3779 MeV [9,10]. In this case the contribution of the ψ to the $\bar{p}p \rightarrow D\bar{D}$ cross section is smaller by about 15%–20%, and, of course, the peak is shifted to the higher energy.

Besides the unsettled parameters of the $\psi(3770)$ resonance, the specific dynamics that generates the nonresonant

part or background of the $D\bar{D}$ interaction affects also the shape of the signal, at least on the quantitative level. In the present model, this background is provided solely by t -channel exchange of the vector mesons ρ , ω , and J/ψ ; see Fig. 2. There are charmonium states not too far from the energy region considered in our study that can contribute and, therefore, could modify the background. First of all this concerns the $\psi(3686)$ which is relatively close to the $D\bar{D}$ threshold and which was found to play an important role in the analyses of the $e^+e^- \rightarrow D\bar{D}$ data [23,27–29]. It could certainly influence the actual shape of the $\psi(3770)$ in the $D\bar{D} \rightarrow D\bar{D}$ and $\bar{p}p \rightarrow D\bar{D}$ reactions. Another resonance that can contribute to the $D\bar{D}p$ wave potential is the $\psi(4040)$. Finally, already below that resonance, the $D^*\bar{D}/D\bar{D}^*$ and $D^*\bar{D}^*$ channels open. Nonetheless, we stress that the qualitative features seen in our results are rather solid because they rely only on known general aspects, namely, first of all unitarity and then the fact that, due to the $\psi(3770)$, the $D\bar{D}$ scattering amplitude in the p wave must have a pole that is located close to the real axis and likewise close to the $D\bar{D}$ threshold.

Differential cross sections for $\bar{p}p \rightarrow D^0\bar{D}^0$ and $\bar{p}p \rightarrow D^+D^-$ at $p_{\text{lab}} = 6.578$ GeV/c are shown in Fig. 6. This momentum corresponds to a total energy of 3773.8 MeV so that the results display the situation practically at the resonance peak. As mentioned before [1] without the $\psi(3770)$ the $D\bar{D}$ pair is produced predominantly in the s wave, cf. the dashed/dotted curves. Of course, this changes drastically once the resonance is included (solid/dash-dotted curves). Still, there is a strong interference between the s and p waves, especially in the D^+D^- case, so that the actual angular distribution does not resemble the one one expects from pure p -wave scattering.

IV. ESTIMATES OF THE CROSS SECTION FOR $\bar{p}p \rightarrow D\bar{D}$

It is possible to provide a rough estimation of the $\bar{p}p \rightarrow D\bar{D}$ cross section around the $\psi(3770)$ peak using experimental information by exploiting the fact that at energies very close to the resonance the reaction amplitude can be well approximated by

$$T^{i,j} \approx \gamma^i \frac{1}{E - m_\psi + i\Gamma_\psi/2} \gamma^j, \quad (4)$$

an expression which is indeed exact at the $\psi(3770)$ pole. Here, γ^i is the dressed vertex function with $i, j = D\bar{D}, \bar{p}p$, and e^+e^- and m_ψ and Γ_ψ the physical mass and width of the $\psi(3770)$, respectively.

The cross section resulting from this amplitude can be cast into the form

$$\sigma_{i \rightarrow j} \approx \frac{(2J+1)}{(2S_i^a+1)(2S_i^b+1)} \frac{4\pi}{q_i^2} \frac{\Gamma_i/2\Gamma_j/2}{(E - m_\psi)^2 + \Gamma_\psi^2/4}, \quad (5)$$

i.e., into the standard Breit–Wigner formula. Here J is the total angular momentum, S_i^a and S_i^b are the spins of the particles in the incoming channel, q_i is the center-of-mass momentum in the incoming channel, and Γ_i and Γ_j are the partial widths for the decay of the $\psi(3770)$ into the channels i and j .

There are cross section data on the reactions $e^+e^- \rightarrow D\bar{D}$ [8] and $e^+e^- \rightarrow \bar{p}p$ [31] in the vicinity of the $\psi(3770)$ resonance. Together with unitarity constraints for $D\bar{D} \rightarrow D\bar{D}$, they allow one to determine all the Γ_i 's needed for estimating the $\bar{p}p \rightarrow D\bar{D}$ cross section. With regard to the $D\bar{D} \rightarrow D\bar{D}$ cross section, we assume for simplicity that $\Gamma_{D\bar{D}} \approx \Gamma_\psi$ —which is anyway consistent with the PDG listing [10]—so that the cross section is given by the unitarity bound. At the energy corresponding to the $\psi(3770)$ resonance, this amounts to $\sigma_{D\bar{D} \rightarrow D\bar{D}} \approx 200$ mb. Assuming that the $I = 1$ p -wave amplitude is small, which is indeed the case in our model (cf. Fig. 3), yields $\sigma_{D^+D^- \rightarrow D^+D^-} \approx 50$ mb. The measured $e^+e^- \rightarrow D^+D^-$ cross section at the $\psi(3770)$ resonance peaks at about 3 nb [8], while the analysis of the $e^+e^- \rightarrow \bar{p}p$ cross section performed in Ref. [31] suggests that the contribution due to the $\psi(3770)$ resonance could amount to either $0.059^{+0.070}_{-0.020}$ or $2.57^{+0.12}_{-0.13}$ pb. Combining those results and using Eq. (5) to determine the various Γ_i 's, we deduce for $\bar{p}p \rightarrow D^+D^-$ a cross section of either $3 \sim 18$ nb or around 350 nb. There is a large uncertainty for the lower value that follows from the BESIII analysis, but, still, one could argue that it is roughly in line with our theory prediction.

As an alternative let us consider also an estimate that follows from a QCD-based perturbative approach to charmonium decays into baryon-antibaryon pairs [32,33]. That approach relies on a factorized expression for the $\psi \rightarrow \bar{p}p$ decay amplitude into a $c\bar{c} \rightarrow \bar{p}p$ annihilation amplitude and the ψ wave function at the origin—see, e.g., Eqs. (4.68)–(4.71) of Ref. [33]. The model dependence regarding the $c\bar{c} \rightarrow \bar{p}p$ annihilation amplitude, which involves at least three gluons in the creation of up and down quark-antiquark pairs, can be eliminated considering the ratio of $\Gamma_{\psi \rightarrow \bar{p}p}$ to $\Gamma_{J/\psi \rightarrow \bar{p}p}$. If, in addition, one assumes that the strong as well as the electronic decays of $\psi(3770)$ proceed predominantly through the 2^3S_1 component of its wave function [recall that the existence of an important 2^3S_1 component comes from the large decay width of $\psi(3770)$ into e^+e^-], one can express $\Gamma_{\psi \rightarrow \bar{p}p}$ in terms of measured quantities:

$$\Gamma_{\psi \rightarrow \bar{p}p} = \left(\frac{1 - 4m_p^2/M_\psi^2}{1 - 4m_p^2/M_{J/\psi}^2} \right)^{\frac{1}{2}} \frac{\Gamma_{\psi \rightarrow e^+e^-}}{\Gamma_{J/\psi \rightarrow e^+e^-}} \Gamma_{J/\psi \rightarrow \bar{p}p}. \quad (6)$$

Using PDG values [10] for the electronic decay widths and for the width of $J/\psi \rightarrow \bar{p}p$, one obtains from Eq. (5) for the cross section $\sigma_{\bar{p}p \rightarrow D^+D^-} \approx 0.2$ nb, due to the $\psi(3770)$,

which is significantly smaller than the value extracted from the BESIII result but also much smaller than our model predictions.

V. SUMMARY

We have presented a study of the reaction $\bar{p}p \rightarrow D\bar{D}$ close to the production threshold with special emphasis on the role played by the $\psi(3770)$ resonance. The work is an extension of a recent calculation by us [1] which is performed within a meson-baryon model where the elementary charm production process is described by baryon exchange and where effects of the interactions in the initial ($\bar{p}p$) and final ($D\bar{D}$) states are taken into account rigorously. The $\psi(3770)$ resonance, which is included in the $D\bar{D}$ FSI in the present calculation, produces a sizeable enhancement in the $\bar{p}p \rightarrow D\bar{D}$ cross

section around the resonance energy. Indeed, our predictions for the total $D\bar{D}$ production cross section in the considered near-threshold region are in the order of 30–250 nb, where the contribution from the $\psi(3770)$ resonance itself amounts to roughly 20–80 nb. Given the magnitude and the shape of the cross section due to the $\psi(3770)$, there should be good chances to measure the pertinent contribution in dedicated experiments which could be performed at FAIR.

ACKNOWLEDGMENTS

This work was partially supported by the Brazilian agencies Conselho Nacional de Desenvolvimento Científico e Tecnológico—CNPq, Grant No. 305894/2009-9, and Fundação de Amparo à Pesquisa do Estado de São Paulo—FAPESP, Grant No. 2013/01907-0.

-
- [1] J. Haidenbauer and G. Krein, *Phys. Rev. D* **89**, 114003 (2014).
 - [2] A. T. Goritschnig, B. Pire, and W. Schweiger, *Phys. Rev. D* **87**, 014017 (2013); **88**, 079903(E) (2013).
 - [3] A. Khodjamirian, C. Klein, T. Mannel, and Y. M. Wang, *Eur. Phys. J. A* **48**, 31 (2012).
 - [4] A. I. Titov and B. Kämpfer, *Phys. Rev. C* **78**, 025201 (2008).
 - [5] B. Kerbikov and D. Kharzeev, *Phys. Rev. D* **51**, 6103 (1995).
 - [6] A. B. Kaidalov and P. E. Volkovitsky, *Z. Phys. C* **63**, 517 (1994).
 - [7] P. Kroll, B. Quadder, and W. Schweiger, *Nucl. Phys.* **B316**, 373 (1989).
 - [8] M. Ablikim *et al.*, *Phys. Lett. B* **668**, 263 (2008).
 - [9] V. V. Anashin *et al.*, *Phys. Lett. B* **711**, 292 (2012).
 - [10] K. A. Olive *et al.* (Particle Data Group), *Chin. Phys. C* **38**, 090001 (2014).
 - [11] W. Erni *et al.*, *arXiv:0903.3905*.
 - [12] U. Wiedner, *Prog. Part. Nucl. Phys.* **66**, 477 (2011).
 - [13] E. Prencipe, *arXiv:1410.5680*.
 - [14] V. Mull and K. Holinde, *Phys. Rev. C* **51**, 2360 (1995).
 - [15] J. Haidenbauer, G. Krein, U.-G. Meißner, and A. Sibirtsev, *Eur. Phys. J. A* **33**, 107 (2007).
 - [16] J. Haidenbauer, G. Krein, U.-G. Meißner, and A. Sibirtsev, *Eur. Phys. J. A* **37**, 55 (2008).
 - [17] J. Haidenbauer, G. Krein, U.-G. Meißner, and L. Tolos, *Eur. Phys. J. A* **47**, 18 (2011).
 - [18] J. Haidenbauer and G. Krein, *Phys. Lett. B* **687**, 314 (2010).
 - [19] J. Haidenbauer, T. Hippchen, K. Holinde, B. Holzenkamp, V. Mull, and J. Speth, *Phys. Rev. C* **45**, 931 (1992).
 - [20] M. Kohno and W. Weise, *Phys. Lett. B* **179**, 15 (1986).
 - [21] D. Lohse, J. W. Durso, K. Holinde, and J. Speth, *Nucl. Phys.* **A516**, 513 (1990).
 - [22] G. Janssen, B. C. Pearce, K. Holinde, and J. Speth, *Phys. Rev. D* **52**, 2690 (1995).
 - [23] Y.-R. Liu, M. Oka, M. Takizawa, X. Liu, W.-Z. Deng, and S.-L. Zhu, *Phys. Rev. D* **82**, 014011 (2010).
 - [24] K. M. Watson, *Phys. Rev.* **88**, 1163 (1952).
 - [25] A. B. Migdal, *JETP* **1**, 2 (1955).
 - [26] X. W. Kang, J. Haidenbauer, and U.-G. Meißner, *Phys. Rev. D* **91**, 074003 (2015).
 - [27] Y.-J. Zhang and Q. Zhao, *Phys. Rev. D* **81**, 034011 (2010).
 - [28] N. N. Achasov and G. N. Shestakov, *Phys. Rev. D* **86**, 114013 (2012).
 - [29] G.-Y. Chen and Q. Zhao, *Phys. Lett. B* **718**, 1369 (2013).
 - [30] N. N. Achasov and G. N. Shestakov, *Phys. Rev. D* **87**, 057502 (2013).
 - [31] M. Ablikim *et al.*, *Phys. Lett. B* **735**, 101 (2014).
 - [32] J. Bolz and P. Kroll, *Eur. Phys. J. C* **2**, 545 (1998).
 - [33] N. Brambilla *et al.*, *arXiv:hep-ph/0412158*.